

Chemical–mechanical polishing behavior of tantalum in slurries containing citric acid and alumina

Jui-Chin Chen, Wen-Ta Tsai*

Department of Materials Science and Engineering, National Cheng Kung University, Tainan, Taiwan, ROC

Received 18 March 2003; accepted in revised form 23 December 2003

Abstract

The effects of H_2O_2 , citric acid and Al_2O_3 content on the electrochemical behavior, surface characteristics and metal removal rates in simulated Ta chemical–mechanical polishing (CMP) have been investigated. Electrochemical measurements indicated that Ta could be easily passivated in all citric acid base slurries prepared in this investigation. The passive film could be removed under CMP condition. The addition of H_2O_2 into the slurries could assist repassivation of Ta under polishing condition. X-ray photoelectron spectroscopy (XPS) revealed that the passive film formed on Ta surface in the citric acid slurries consisted of Ta_2O_5 and Ta–O–H. The presence of H_2O_2 enhanced the formation of Ta_2O_5 on Ta surface. The removal rate obtained in the simulated CMP investigation increased with the amount of Al_2O_3 , either in DI water or in the 0.01 M citric acid + 9 vol.% H_2O_2 slurries. The surface roughness of Ta after CMP in 0.01 M citric acid + 9 vol.% H_2O_2 slurries was higher than that in DI water base slurries when the Al_2O_3 content was low. A significant reduction in surface roughness combined with a high removal rate could be obtained if the Al_2O_3 content in the 0.01 M citric acid + 9 vol.% H_2O_2 slurries was increased to above 10 wt.%.

© 2004 Elsevier B.V. All rights reserved.

Keywords: Tantalum; Chemical–mechanical polishing (CMP); Hydrogen peroxide; Citric acid; Alumina

1. Introduction

Chemical–mechanical polishing (CMP) is a promising means of technique for removing excess copper and planarizing the surface on a global scale. Much effort has been devoted to the study of Cu CMP with some different mechanisms proposed [1–4]. In order to successfully integrate Cu into ICs, an appropriate diffusion barrier layer, such as Ta [5–8], Ta_2N [7,8], TaN [8] or amorphous Ta–Si–N [6], all of which are thermodynamically stable with respect to Cu, is usually applied. However, studies on the CMP behavior of Ta and its nitrides are fewer [9–12] than those of Cu.

The effects of abrasive particles and oxidant addition on the polishing rate in de-ionized (DI) water were investigated with reference to Ta CMP [9]. Under an applied downward

pressure of 6.3 psi and a rotation of a table at 90 rev./min, Hariharaputhiran et al. [9] reported that no measurable polishing rate was obtained in the absence of abrasive particles (either alumina or fumed silica). The addition of 3 wt.% alumina and Aerosil silica abrasive particles raised the polishing rate to 67 nm/min and 74 nm/min, respectively. However, the addition of an oxidant, such as $Fe(NO_3)_3$ or $Cu(NO_3)_2$, among others, reduced the Ta polishing rate in DI water that contained abrasive particles. The adverse effect of adding H_2O_2 , which reduced the polishing rate in Ta CMP, has also been observed in DI water that contained fumed amorphous silica. This result was in contrast to that found for Cu CMP [10]. Li and Babu [10] indicated that the addition of H_2O_2 presumably caused the formation of a hard oxide film on the Ta surface, which could thus decrease the polishing rate. Kuiry et al. examined the effect of pH on Ta CMP [11]. They found that the etching rate of Ta increased with pH in the slurry of 3% alumina abrasive particles. They also indicated that an impervious oxide layer was found in a solution of 5% H_2O_2 at pH 2, while a porous layer was formed on Ta with 5% H_2O_2 at pH 12. The dependence of

* Corresponding author. Tel.: +886-6-2757575 ext. 62927; fax: +886-6-2754395.

E-mail address: wtsai@mail.ncku.edu.tw (W.-T. Tsai).

the polishing rate on the slurry pH was probably due to the different oxide formed on the Ta surface. A similarly pH-dependent polishing rate was observed in a 2% KIO_3 base slurry that contained silica abrasive [12].

The slurry used in CMP always incorporates chelating agents, whose roles in CMP should not be ignored. However, the mentioned investigation [9] of Ta CMP was mainly conducted in DI water without involving chelating agents. Accordingly, the effect of citric acid, commonly employed in Al or Cu CMP, on the Ta CMP polishing rate was explored. The effect of abrasive particle content on the polishing rate was also studied. Electrochemical measurements, X-ray photoelectron spectroscopy (XPS) and atomic force microscopy (AFM) were performed to elucidate the passivation/breakdown behavior and the change in the surface morphology in Ta CMP.

2. Experimental

A pure Ta rod (99.95%), with a diameter of 2.5 cm, was sliced into 0.8 cm thick disks. Each disk was mounted in epoxy resin with one surface exposed. The exposed surface was ground using SiC paper to a grit of 800. Then, three discs, whose axes were at 120° to each other, were mounted onto the carrier of a polisher for subsequent electrochemical testing and removal rate measurements.

The polisher was designed to simulate the CMP mechanism [4]. Fig. 1 demonstrates the schematic diagram of this polisher. This polisher consisted of a lower platen and an

upper carrier with diameters of 20.3 cm and 7.6 cm, respectively. A loading device was attached to the upper carrier. The lower platen was bonded with a tank to hold the slurry during polishing. The platen and the carrier rotated in opposite directions at 100 rev./min and 10 rev./min, respectively. A downward stress of 3 psi was applied to the specimens in the carrier. A Rodel IC-1400 polished pad was attached to the platen. Then all the electrochemical tests and removal rate measurements were performed in this polisher.

Two different types of slurries, namely DI water and citric acid bases, were used in this investigation. The concentrations of citric acid (CA) were 0.008, 0.01 and 0.5 M. Al_2O_3 powders with an average size of $0.05 \mu\text{m}$ were used as the abrasive particles. Their contents varied from 0 to 15 wt.%. H_2O_2 at a concentration of 9 vol.% was added to some slurry as the oxidizing agent.

The potentiodynamic polarization curves and open circuit potentials were measured under stationary conditions or during CMP. An EG&G model 362 electrochemical system connected to a Yokogawa LR4110 recorder, was used to monitor the potential and the current during testing. A saturated calomel electrode (SCE) and a platinum sheet were used as the reference electrode and the counter electrode, respectively.

The weight loss of the specimen after simulated CMP for 3 h was measured. An analytical precision microbalance (Sartorius CP 225D electronic microbalance) with an accuracy to $\pm 0.1 \text{ mg}$ was used for weight change measurement. The total weight loss consisted of both from Ta and epoxy resin. Knowing the densities and the area ratio between Ta

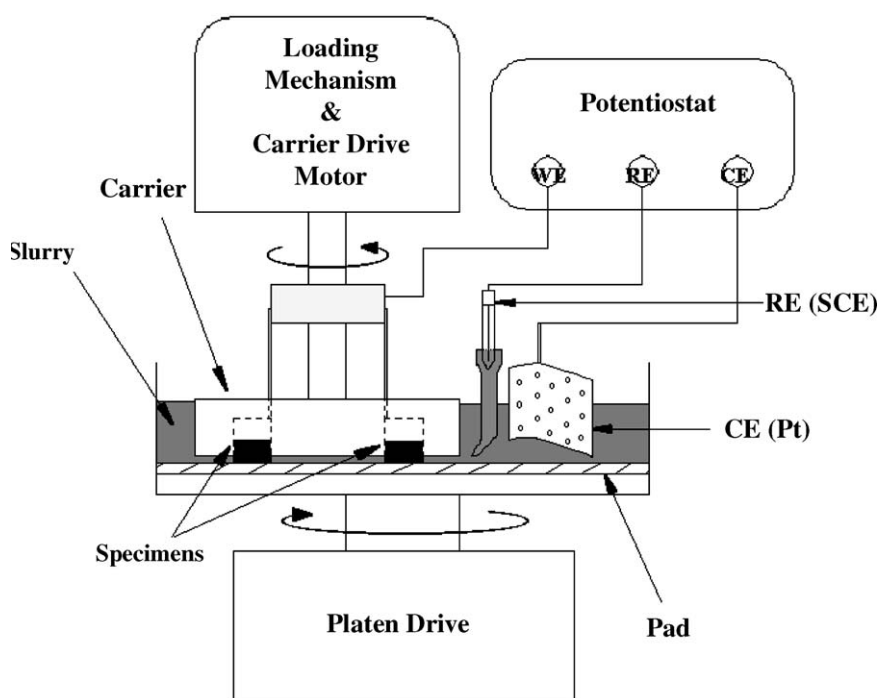


Fig. 1. Schematic diagram of the apparatus used in electrochemical and CMP tests.

and epoxy resin, the weight loss of Ta could then be determined. The total removal rate (R_t), in terms of $\text{\AA}/\text{min}$, was thus calculated and averaged from the three specimens.

X-Ray photoelectron spectroscopy (XPS) was employed for surface chemical analysis. The XPS analysis was performed with a Fison (VG) ESCA210 instrument. Excitation was performed by Al $K\alpha$ radiation ($h\nu=1486.6$ eV). All spectra were calibrated with respect to the C 1S electron peak at 284.6 eV. Furthermore, the background of the XPS data was subtracted before conducting chemical analysis. XPS spectra curve fitting analysis was performed by employing the Origin 6.0 software developed by OriginLab Corporation.

A NT-MDT P7LS contact mode of atomic force microscope (AFM) was used for surface examination after CMP. In each slurry, the CMP was repeated for three times. On each specimen, two AFM measurements were performed. The surface roughness was thus averaged from six measurements. The arithmetic mean surface roughness (R_a) was also evaluated by AFM. These parameters [13] are defined as,

$$R_c = \frac{1}{N_x N_y} \sum_{i=1}^{N_x} \sum_{j=1}^{N_y} z_{ij}$$

$$R_a = \frac{1}{N_x N_y} \sum_{i=1}^{N_x} \sum_{j=1}^{N_y} |z| \quad z = z_{ij} - R_c$$

where z_{ij} is the height of parallel to the Z axis. N_x and N_y are the number of points along the X and Y axes.

3. Results and discussion

3.1. Electrochemical behavior

Fig. 2 depicts the effects of the concentration of citric acid on the potentiodynamic polarization behavior of Ta in the slurries containing 1 wt.% Al_2O_3 . Under load-free and static conditions, the polarization curves exhibited similar features in both 0.008 and 0.5 M CA (citric acid) slurries, except that the corrosion potential in the latter was slightly higher than that in the former. A wide passive range with a passive current density of $1.4 \times 10^{-5} \text{ A}/\text{cm}^2$ were observed, indicating that Ta could be easily passivated in both slurries.

Under simulated CMP with an applied stress of 3 psi, as revealed in Fig. 2, the plateaus of the passive range in the polarization curves disappeared and the corrosion potentials in both slurries shifted slightly in the negative direction. The loss of passivity implied that the passive film could be removed by mechanical force. As shown in Fig. 2, under simulated CMP conditions, the anodic current in the 0.5 M

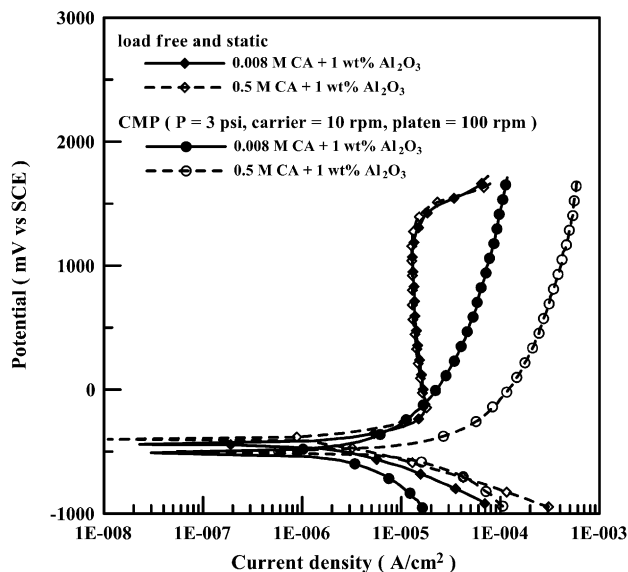


Fig. 2. Effect of concentration of citric acid on the potentiodynamic polarization of Ta in various solutions with 1 wt.% Al_2O_3 under various conditions.

CA slurry was higher than that in the 0.008 M CA slurry. Besides, as an oxidizing agent, citric acid can also offer a chelating effect on many metallic ions. At a low concentration of citric acid (say 0.008 M), the amount of chelating agent was probably insufficient to fix all of the dissolved Ta ions. As a result, the un-chelated Ta ions tended to form the oxide and partially passivated the surface. When the concentration of citric acid was high (ex. 0.5 M), most of the dissolved Ta ions chelated with citric acid could be carried away, with the aid of flowing slurry in CMP. In such a case, repassivation was retarded, resulting in a higher anodic current density, as revealed in Fig. 2.

Fig. 3 presents the effect of H_2O_2 in the citric acid slurry containing 1 wt.% Al_2O_3 on the polarization behavior of Ta. Both under static conditions and CMP, the addition of 9 vol.% H_2O_2 to 0.5 M CA + 1 wt.% Al_2O_3 slurry was found to increase the corrosion potential. Under static conditions, a narrower passive range in the polarization curve was observed when H_2O_2 was added. Under CMP conditions, as expected, the mechanical force helped to remove the passive film with or without H_2O_2 addition. However, the anodic current density in the citric acid base slurry that contained H_2O_2 was lower than that in the slurry without H_2O_2 . Since H_2O_2 is a strong oxidant, repassivation of Ta was promoted in the slurry with H_2O_2 , even though the concentration of citric acid was high. Similar to that found in 0.5 M CA base slurries, the effect of H_2O_2 addition in reducing the anodic current density was also observed in the 0.008 M CA slurries.

The effect of H_2O_2 addition to the citric acid base slurries on the change of the open circuit potential was studied. Fig. 4 shows the open circuit potential vs. time plots before and after H_2O_2 addition under various conditions. Under static

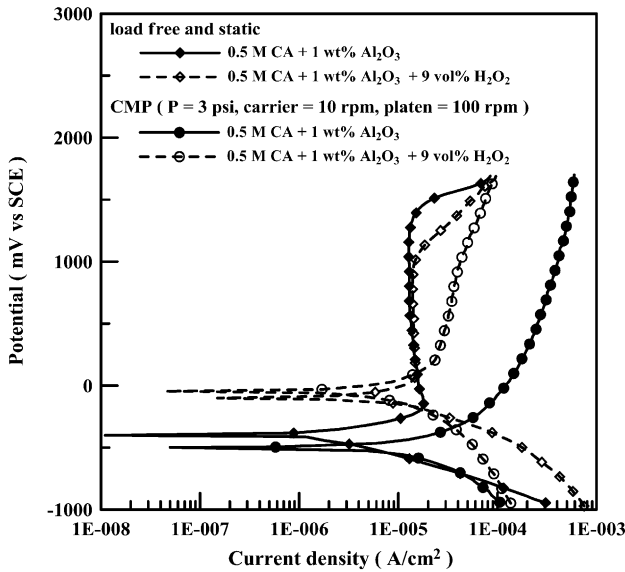


Fig. 3. Effect of H₂O₂ on the potentiodynamic polarization of Ta in 0.5 M CA + 1 wt.% Al₂O₃ slurries under various conditions.

conditions and in the absence of H₂O₂, the open circuit potential slightly increased with time in the slurry with either 0.008 or 0.5 M CA. In the 0.5 M CA slurry, the open circuit potential was higher than that in the 0.008 M CA slurry. The high concentration of H⁺ was the primary cause of the higher open circuit potential in the former slurry. Under CMP conditions, however, the open circuit potential decreased with time, and became stable until approximately -580 mV in both slurries. The decrease in the open circuit potential was due to the breakdown of the passive film during CMP.

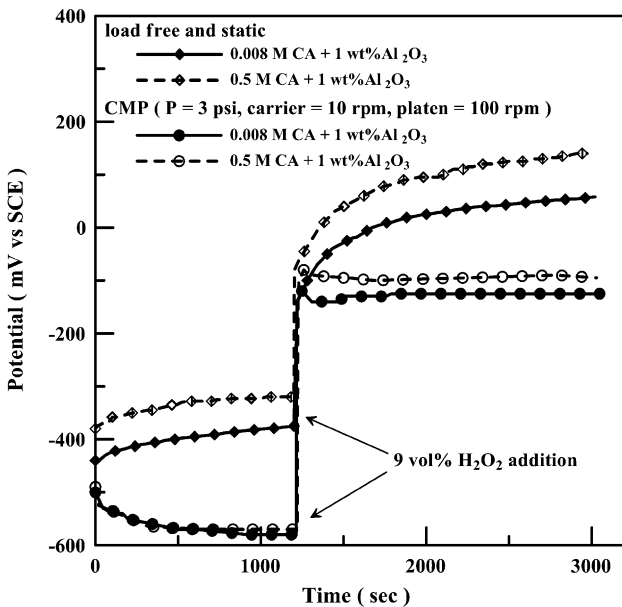


Fig. 4. Effect of H₂O₂ on the open circuit potentials of Ta in citric acid solution containing 1 wt.% Al₂O₃.

After 9 vol.% H₂O₂ was added, a significant increase in the open circuit potential, as depicted in Fig. 4, was observed in each slurry, with or without polishing. Under static conditions, the high oxidizing power of H₂O₂ assisted the passivation of Ta and significantly raised the potential. Under CMP conditions, the potential was lower than that under static conditions, in each slurry. The rather high open circuit potential observed under CMP conditions indicated that a passive film could still be formed under polishing conditions if H₂O₂ was added.

3.2. XPS analysis

The surface compositions of Ta immersed in different slurries for 60 min were examined by XPS. Fig. 5 presents the XPS envelope of Ta 4f_{7/2} and 4f_{5/2} for the as-ground Ta (Fig. 5a) and that after immersion in DI water for 60 min (Fig. 5b). The peaks at 21.3 and 23 eV correspond to metallic Ta 4f_{7/2} and metallic Ta 4f_{5/2} spectra [14], and the peaks at 26.1 eV for Ta 4f_{7/2} and 28 eV for Ta 4f_{5/2} demonstrate the formation of Ta₂O₅ [15,16]. The peaks at 23.1 eV and 24.3 eV (Ta 4f_{7/2} and Ta 4f_{5/2}) was probably associated with a Ta–O–H type complex [11]. Clearly, the surface film was composed of Ta₂O₅ and tantalum hydroxide when Ta was immersed in DI water. The high intensities of the peaks associated with metallic Ta indicated that the surface film might be thin or less continuous. Similar results were obtained when Ta was immersed in DI water that contained 1 wt.% Al₂O₃. The effect of H₂O₂ on the changes of the surface compositions of Ta in various slurries was also evaluated by XPS. When 9 vol.% H₂O₂

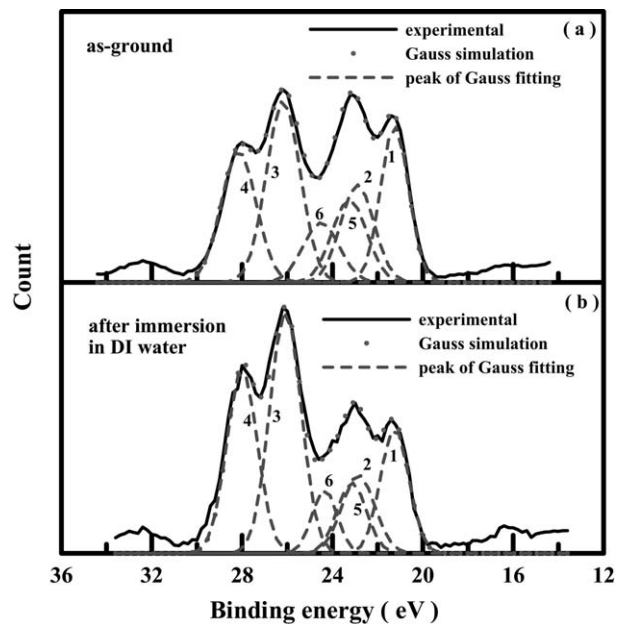


Fig. 5. Peak fitted XPS envelope of Ta 4f for Ta (a) as-ground and (b) after immersed in DI water for 60 min, where metallic Ta: (1) Ta 4f_{7/2} and (2) Ta 4f_{5/2}; Ta₂O₅: (3) Ta 4f_{7/2} and (4) Ta 4f_{5/2}; Ta–O–H type complex: (5) Ta 4f_{7/2} and (6) Ta 4f_{5/2}.

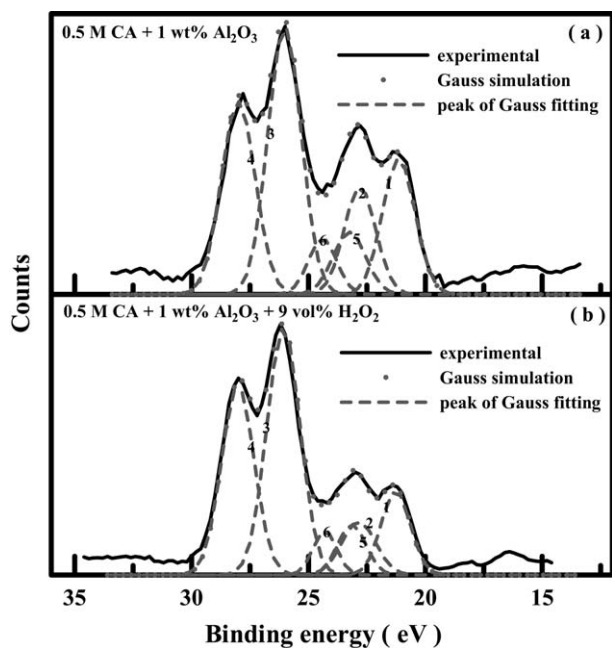


Fig. 6. XPS spectra of Ta $4f_{7/2}$ and $4f_{5/2}$ after Ta immersion in (a) 0.5 M CA + 1 wt.% Al_2O_3 and (b) 0.5 M CA + 9 vol.% H_2O_2 + 1 wt.% Al_2O_3 slurries for 60 min, where metallic Ta: (1) Ta $4f_{7/2}$ and (2) Ta $4f_{5/2}$; Ta_2O_5 : (3) Ta $4f_{7/2}$ and (4) Ta $4f_{5/2}$; Ta–O–H type complex: (5) Ta $4f_{7/2}$ and (6) Ta $4f_{5/2}$.

was added to either the DI water base or the citric acid base slurry, the peaks that represent Ta_2O_5 were higher than those associated with metallic Ta. Fig. 6 shows an example of the XPS spectra on the surface of Ta immersed in 0.5 M CA + 1 wt.% Al_2O_3 slurry without (Fig. 6a) and with (Fig. 6b) 9 vol.% H_2O_2 added. The higher peak ratio between Ta_2O_5 and metallic Ta indicated that H_2O_2 promoted the formation of Ta_2O_5 . Table 1 summarizes the effect of H_2O_2 on the peak ratios between Ta_2O_5 and metallic Ta for Ta $4f_{5/2}$ and Ta $4f_{7/2}$ after immersion in DI water and different slurries.

3.3. Removal rate and surface morphology

Under simulated CMP, the removal rates of Ta in DI water and in various slurries that contained 1 wt.% Al_2O_3 abrasive particles were estimated, which are presented in

Table 2. In DI water, in the absence of Al_2O_3 abrasive particles, the removal rate could not be detected. With the addition of 1 wt.% Al_2O_3 abrasive particles to DI water, without the addition of H_2O_2 , the measured removal rate was 26 $\text{\AA}/\text{min}$. In a similar study conducted by Jindal et al. [17], the removal rate of Ta in 3 wt.% Al_2O_3 slurry at a stress of 6 psi was approximately 90 $\text{\AA}/\text{min}$. Such high removal rate was probably attributed to the presence of more amounts of abrasive particles and the high stress compared to the present study.

In other slurries with 1 wt.% Al_2O_3 particles, however, no measurable weight losses were detected (Table 2). The polarization curves shown in Fig. 3 show that Ta could be passivated in citric acid slurries even in the absence of H_2O_2 . Furthermore, as revealed by XPS analyses, the presence of H_2O_2 in the slurries causes the formation of a thicker and more uniform Ta_2O_5 on the surface. Apparently, the Ta_2O_5 film was hard enough to resist abrasion in the slurries that contained 1 wt.% Al_2O_3 particles at a stress of 3 psi.

Surface morphologies of Ta before and after simulated CMP were examined by AFM. Fig. 7 presents the AFM image of Ta surface ground using SiC paper to a grit of 800. A rough surface with a parallel pattern due to scratching during grinding was observed. On the testing area, the surface roughness (R_a) was 127 nm. Following the simulation of CMP in DI water, the corresponding AFM image revealed that the parallel scratches remained on the surface with only a slight reduction in the surface roughness, as compared with that of the as-ground specimen.

Fig. 8 displays the AFM image of the Ta surface after simulated CMP in the 1 wt.% Al_2O_3 slurry. A significant reduction in surface roughness was noticed. The value of R_a was 22 nm. As pointed out earlier, the corresponding removal rate measured in this slurry was 26 $\text{\AA}/\text{min}$, which was lower than that of Cu CMP [4]. Nevertheless, planarization could be achieved in such a slurry.

In 1 wt.% Al_2O_3 slurries in the presence of CA with/without H_2O_2 , the surface roughness could only be reduced slightly as compared with that obtained in DI water. Fig. 9 gives an example of the AFM image of Ta after simulated CMP in 0.008 M CA + 1 wt.% Al_2O_3 slurry. Though the image revealed a feature associated with chemical attack of

Table 1

Effect of H_2O_2 on the XPS peak intensity ratios between oxide and metallic Ta for Ta $4f_{5/2}$ and Ta $4f_{7/2}$ after immersion in DI water and different slurries for 60 min

Solution composition	Ratio of $\text{Ta}_2\text{O}_5/\text{Ta}$			
	Ta ($4f_{5/2}$)		Ta ($4f_{7/2}$)	
	Without H_2O_2	With H_2O_2	Without H_2O_2	With H_2O_2
As-prepared	1.4	–	1.4	–
DI water	2.2	–	2.1	–
1 wt.% Al_2O_3	2.0	3.3	2.1	3.3
0.008 M CA + 1 wt.% Al_2O_3	1.9	3.3	2.0	3.5
0.5 M CA + 1 wt.% Al_2O_3	1.9	3.4	2.0	3.3

Table 2

Effect of 1 wt.% Al_2O_3 in various slurries on removal rate (R_t) and average roughness (R_a) of Ta, after simulated CMP ($P=3$ psi, carrier=10 rev./min, platen=100 rev./min)

Slurry	R_t ($\text{\AA}/\text{min}$)	R_a (nm)
Initial surface before CMP (#800)	–	127
DI water (pH=6.3)	ND*	115
1 wt.% Al_2O_3 (pH=4.4)	26 ± 5	22
1 wt.% Al_2O_3 +9 vol.% H_2O_2 (pH=4.1)	ND*	71
0.008 M CA+1 wt.% Al_2O_3 (pH=2.74)	ND*	73
0.5 M CA+1 wt.% Al_2O_3 (pH=1.54)	ND*	76
0.008 M CA+1 wt.% Al_2O_3 +9 vol.% H_2O_2 (pH=2.56)	ND*	90
0.5 M CA+1 wt.% Al_2O_3 +9 vol.% H_2O_2 (pH=1.34)	ND*	93

*Not Detected.

the surface, the metal removal rate was not measurable and the values of the parameters that reflect surface roughness were still very large. Similar observations were found in other slurries that contained CA with/without H_2O_2 . Tables 2 and 3 show all the surface roughness parameters determined by AFM.

The effect of Al_2O_3 particle content on the removal rate of Ta under simulated CMP at 3 psi in DI water and in 0.01 M CA+9 vol.% H_2O_2 slurries, were evaluated. Table 3 presents the results. Varying the Al_2O_3 content from 1 to 15 wt.% in DI water increased the removal rate from 26 to 118 $\text{\AA}/\text{min}$. In DI water with 15 wt.% Al_2O_3 particles, a slight reduction in the polishing rate was observed when 9 vol.% H_2O_2 was added. The addition of H_2O_2 might assist repassivation on the Ta surface, although less than that in the slurry with 1 wt.% Al_2O_3 abrasive particles.

In citric acid base slurries, the removal rate was lower than that in DI water base slurries. As shown in Table 3, the removal rates of Ta in 0.01 M CA+15 wt.% Al_2O_3 and 0.5 M CA+15 wt.% Al_2O_3 slurries were less than that in plain 15 wt.% Al_2O_3 slurry. A further reduction in the metal removal rate was observed when H_2O_2 was added to the citric acid base slurries, as determined by comparing the results obtained in 0.01 M CA+15 wt.% Al_2O_3 slurries with and without H_2O_2 . As revealed in Table 3, the removal rate was trivial when the Al_2O_3 content was less than 3 wt.% in 0.01 M CA+9 vol.% H_2O_2 base slurries. At above 5

wt.%, however, the removal rate increased with increasing Al_2O_3 content in these slurries. In general, the removal rates were lower than those in plain Al_2O_3 slurries (without citric acid and H_2O_2) with the same amount of solid particles.

As reported in the literature [4,18], citric acid plays a beneficial role in CMP of Al and Cu. However, as found herein, a reduction in the polishing rate has been noted in Ta CMP in the presence of citric acid. Whether the chelating effect of citric acid modifies the polishing mechanism is not understood and needs further study.

Fig. 10 shows the effect of Al_2O_3 content on the removal rate and the arithmetic mean surface roughness (R_a). In both DI water and 0.01 M CA+9 vol.% H_2O_2 base slurries, the removal rate increased with Al_2O_3 content. In DI water base slurries, a low surface roughness could be attained. However, roughness slowly increased with Al_2O_3 content up to 7 wt.%. In 0.01 M CA+9 vol.% H_2O_2 base slurries; on the contrary, the surface roughness was reduced to the level determined in DI water base slurries. In CMP, both mechanical abrasion and chemical dissolution would modify the surface morphology. The combined mechanical and chemical effects would lead to the existence of a critical content of abrasive particles beyond which a reduced surface roughness associated with a satisfactory removal rate could be obtained. The results shown in Fig. 10 demonstrate that the Al_2O_3 content should exceed 10 wt.% to reach a high removal rate and a low surface

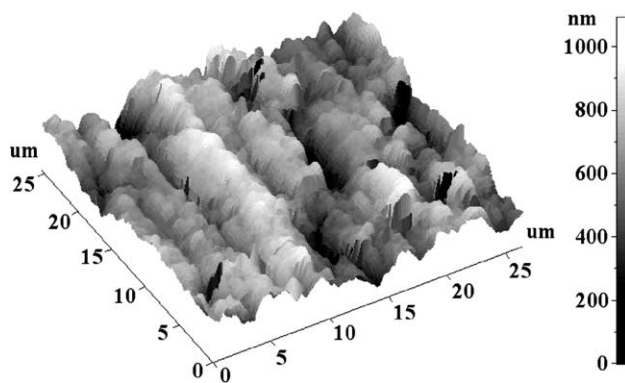


Fig. 7. AFM Surface morphology of as-ground Ta using SiC polishing paper.

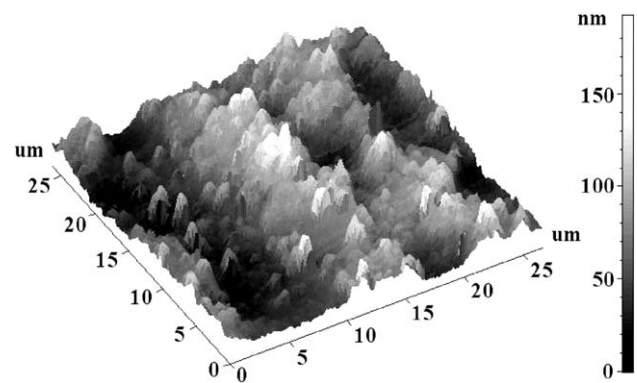


Fig. 8. AFM Surface morphology of Ta after simulated CMP in 1 wt.% Al_2O_3 slurry for 3 h.

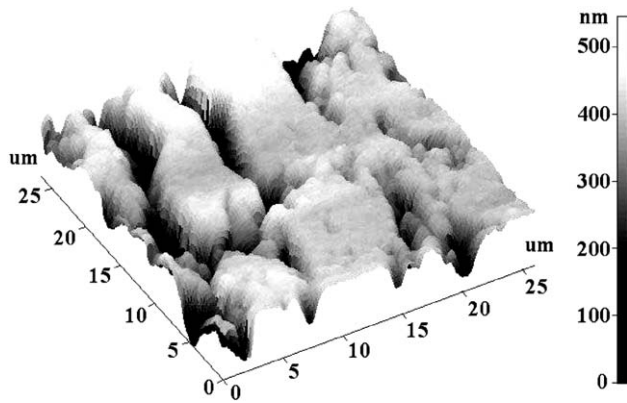


Fig. 9. AFM Surface morphology of Ta after simulated CMP in 0.008 M CA + 1 wt.% Al_2O_3 slurry for 3 h.

roughness in both DI water and 0.01 M + 9 vol.% H_2O_2 base slurries. It was noted to found that the surface roughness reached a value close to that of the average particle size of approximately 50 nm for Al_2O_3 powders.

4. Conclusions

1. The potentiodynamic polarization curves obtained in load free and static condition showed that Ta could be passivated in citric acid base slurries, either with or without H_2O_2 addition.
2. Under CMP condition, a substantial increase in the anodic current density was observed in the absence of H_2O_2 . However, the presence of H_2O_2 in the citric acid slurry caused a reduction of the anodic current density, but still higher than that obtained in load free and static condition.
3. Under static condition, a higher open circuit potential was observed in the slurry with a higher concentration of citric acid, which was further increased with the presence of H_2O_2 . In the absence of H_2O_2 , however, the open

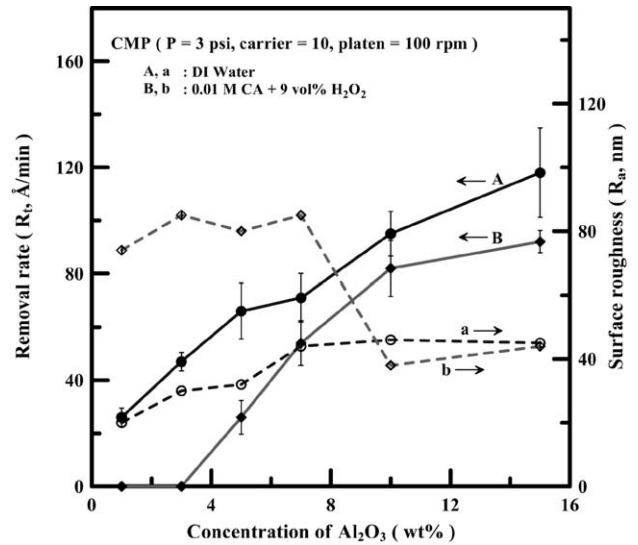


Fig. 10. Effect of Al_2O_3 content on the removal rate and arithmetic mean surface roughness following simulated Ta CMP in DI water and in 0.01 M CA + 9 vol.% H_2O_2 base slurries.

circuit was almost the same in the slurries with 0.008 and 0.5 M citric acid under CMP condition.

4. XPS results showed that Ta_2O_5 and Ta—O—H were formed on the as-ground Ta as well as that after immersion in DI water for 60 min. In H_2O_2 -containing slurries, a noticeable increase in the peak intensities for Ta_2O_5 was found, indicating the occurrence of enhanced passivation with Ta_2O_5 formation.
5. In both citric acid free and in 0.01 M citric acid + 9 vol.% H_2O_2 slurries, the metal removal rate increased with increasing amount of Al_2O_3 abrasive particles in Ta CMP. However, the presence of citric acid and H_2O_2 resulted in a reduced the polishing rate, compared with that in DI water slurry.
6. A high metal removal rate combined with a low surface roughness could be obtained in either DI water or 0.01 M

Table 3

Effect of alumina content on the removal rate (R_t) and the average roughness (R_a) of Ta in simulated CMP ($P=3$ psi, carrier = 10 rev./min, platen = 100 rev./min)

Slurry	R_t ($\text{\AA}/\text{min}$)	R_a (nm)
1 wt.% Al_2O_3 (pH=4.4)	26 ± 5	22
3 wt.% Al_2O_3 (pH=4.4)	47 ± 5	30
5 wt.% Al_2O_3 (pH=4.4)	66 ± 15	32
7 wt.% Al_2O_3 (pH=4.4)	71 ± 13	44
10 wt.% Al_2O_3 (pH=4.4)	95 ± 12	46
15 wt.% Al_2O_3 (pH=4.4)	118 ± 20	45
15 wt.% Al_2O_3 + 9 vol.% H_2O_2 (pH=4.2)	113 ± 19	—
0.01 M CA + 15 wt.% Al_2O_3 (pH=3.7)	110 ± 20	—
0.5 M CA + 15 wt.% Al_2O_3 (pH=1.8)	100 ± 13	—
0.01 M CA + 1 wt.% Al_2O_3 + 9 vol.% H_2O_2 (pH=2.4)	ND*	74
0.01 M CA + 3 wt.% Al_2O_3 + 9 vol.% H_2O_2 (pH=2.5)	ND*	85
0.01 M CA + 5 wt.% Al_2O_3 + 9 vol.% H_2O_2 (pH=2.7)	26 ± 9	80
0.01 M CA + 7 wt.% Al_2O_3 + 9 vol.% H_2O_2 (pH=2.9)	54 ± 12	85
0.01 M CA + 10 wt.% Al_2O_3 + 9 vol.% H_2O_2 (pH=3.3)	82 ± 15	38
0.01 M CA + 15 wt.% Al_2O_3 + 9 vol.% H_2O_2 (pH=3.4)	92 ± 6	44

*Not Detected.

citric acid +9 vol.% H₂O₂ slurry when the Al₂O₃ abrasive content exceeded 10 wt.%.

Acknowledgments

The authors would like to thank the National Science Council of the Republic of China for financially supporting this research under Contract No. NSC 90-2216-E-006-042.

References

- [1] S. Kondo, N. Sakuma, Y. Homma, N. Ohashi, *The Electrochemical Society Proceedings Series*, Pennington, PV 98-6 NJ, 1998 pp. 195–205.
- [2] D. Zeidler, Z. Stavreva, M. Plotner, K. Drescher, *Microelectron. Eng.* 33 (1997) 259–265.
- [3] R.J. Gutmann, J.M. Steigerwald, L. You, D.T. Price, J. Neiyneck, D.J. Duquette, S.P. Murarka, *Thin Solid Film* 270 (1995) 596–600.
- [4] J.C. Chen, W.T. Tsai, submitted to *J. Electrochem. Soc.*
- [5] C.A. Chang, *J. Appl. Phys.* 67 (12) (1990) 7348–7350.
- [6] E. Kolawa, J.S. Chen, J.S. Reid, P.J. Pokela, M.A. Nicolet, *J. Appl. Phys.* 70 (3) (1991) 1369–1373.
- [7] K. Holloway, P.M. Fryer, C. Cabral Jr., J.M.E. Harper, P.J. Bailey, K.H. Kelleher, *J. Appl. Phys.* 71 (11) (1992) 5433–5444.
- [8] K.H. Min, K.C. Chun, K.B. Kim, *J. Vac. Sci. Technol. B* 14 (5) (1996) 3263–3269.
- [9] M. Hariharaputhiran, Y. Li, S. Ramarajan, S.V. Babu, *Electrochem. Solid-St. Lett.* 3 (2) (2000) 95–98.
- [10] Y. Li, S.V. Babu, *J. Mater. Res.* 16 (4) (2001) 1066–1073.
- [11] S.C. Kuiry, S. Seal, W. Fei, J. Ramsdell, V.H. Desai, Y. Li, S.V. Babu, B. Wood, *J. Electrochem. Soc.* 150 (1) (2003) C36–43.
- [12] Y. Li, S.V. Babu, *Electrochem. Solid-St. Lett.* 4 (2) (2001) G20–22.
- [13] International standard ISO 4287, 1997, p. 12.
- [14] J.F. Moulder, J. Chastain, R.C. King, *Handbook of X-Ray Photoelectron Spectroscopy Physical Electronics and Minn. Eden Prairie*, 1995, p. 171.
- [15] E. Atanassova, T. Dimitrova, J. Koprinarova, *Appl. Surf. Sci.* 84 (1995) 193–202.
- [16] E. Atanassova, D. Spassov, *Appl. Surf. Sci.* 135 (1998) 71–82.
- [17] A. Jindal, S. Hegde, S.V. Babu, *Electrochem. Solid-St. Lett.* 5 (7) (2002) G48–50.
- [18] H.S. Kuo, W.T. Tsai, *Mater. Chem. Phys.* 69 (2001) 53–61.